

Dalton Transactions

Accepted Manuscript



This is an *Accepted Manuscript*, which has been through the Royal Society of Chemistry peer review process and has been accepted for publication.

Accepted Manuscripts are published online shortly after acceptance, before technical editing, formatting and proof reading. Using this free service, authors can make their results available to the community, in citable form, before we publish the edited article. We will replace this *Accepted Manuscript* with the edited and formatted *Advance Article* as soon as it is available.

You can find more information about *Accepted Manuscripts* in the [Information for Authors](#).

Please note that technical editing may introduce minor changes to the text and/or graphics, which may alter content. The journal's standard [Terms & Conditions](#) and the [Ethical guidelines](#) still apply. In no event shall the Royal Society of Chemistry be held responsible for any errors or omissions in this *Accepted Manuscript* or any consequences arising from the use of any information it contains.

**Organization and intramolecular charge-transfer enhancement in tripodal
tris[(pyridine-4-yl)phenyl]amine push-pull molecule by intercalation into layered
materials bearing acidic functionalities**

Klára Melánová,^a Daniel Cvejn,^b Filip Bureš,^b Vítězslav Zima,^{a*} Jan Svoboda,^a Ludvík Beneš,^c
Tomáš Mikysek,^d Oldřich Pytela,^b Petr Knotek^c

^a *Institute of Macromolecular Chemistry, AS CR, Heyrovsky sq. 2, 162 06 Prague 6, Czech Republic*

^b *Institute of Organic Chemistry and Technology, Faculty of Chemical Technology, University of Pardubice, 532 10 Pardubice, Czech Republic*

^c *Joint Laboratory of Solid State Chemistry, Faculty of Chemical Technology, University of Pardubice, 532 10 Pardubice, Czech Republic*

^d *Department of Analytical Chemistry, Faculty of Chemical Technology, University of Pardubice, 532 10 Pardubice, Czech Republic*

*To whom correspondence should be addressed. E-mail: vitezslav.zima@upce.cz (V. Zima)

†Electronic supplementary information (ESI) available: Preparation and characterization of **TPPA** and **MeTPPA**, UV-Vis absorption spectra of **TPPA** and **MeTPPA**, ¹H NMR and ¹³C NMR APT spectrum of **MeTPPA**, thermal powder X-ray patterns of **ZrP·TPPA** and **ZrSPP·TPPA**, IR spectrum of partially protonated TPPA, deconvoluted UV-Vis spectra of **ZrP·TPPA** and **ZrSPP·TPPA**, UV-Vis spectrum of **ZrP·TPPA** treated with HCl.

Abstract

Two new intercalates of tris[4-(pyridin-4-yl)phenyl]amine (**TPPA**) with zirconium hydrogen phosphate and zirconium 4-sulfophenylphosphonate having formulae $\text{Zr}(\text{HPO}_4)_2 \cdot 0.21(\text{C}_{33}\text{H}_{24}\text{N}_4) \cdot 2.5\text{H}_2\text{O}$ and $\text{Zr}(\text{HO}_3\text{SC}_6\text{H}_4\text{PO}_3)_{1.3}(\text{C}_6\text{H}_4\text{PO}_3)_{0.7} \cdot 0.35(\text{C}_{33}\text{H}_{24}\text{N}_4) \cdot 2.5\text{H}_2\text{O}$ were prepared and characterized by thermogravimetry, IR spectroscopy, and powder X-ray diffraction. The **TPPA** molecule has been selected as a model tripodal push-pull system with three peripheral basic centers that may undergo protonation. Their protonation/quaternization afforded **HTPPA/MeTPPA** molecules with enhanced intramolecular charge-transfer (ICT), which has been documented by the electrochemical measurements, UV-Vis spectra and calculated properties such as the HOMO/LUMO levels and the first and second hyperpolarizabilities. Intercalation of **TPPA** into layered zirconium hydrogen phosphate and zirconium 4-sulfophenylphosphonate led to its significant organization and protonation as shown by the IR spectra. From the powder X-ray data we can deduce that the **TPPA** molecules are placed in the interlayer space of both hosts by anchoring two peripheral nitrogen atoms to one host layer and the opposite pyridine-4-yl terminus to other neighboring layer. In zirconium 4-sulfophenylphosphonate, the **TPPA** molecules are oriented perpendicularly, while in zirconium phosphate these molecules are slanted with respect to the layers of the host. On dehydration by heating the interlayer distance of the intercalate decreases, which indicates a further slanting of the **TPPA** molecules. It follows from the UV-Vis spectra that **TPPA** is present in both intercalates in an equilibrium of protonated and non-protonated forms. The described materials represent the first case when a tripodal push-pull system was incorporated in a system with restricted geometry with the aim to influence its optical properties.

Introduction

Organic π -conjugated compounds are of interest for a wide scientific community due to their unique properties and miscellaneous applications. In an organic molecule with a D- π -A arrangement, an intramolecular charge-transfer (ICT) from the donor (D) to the acceptor (A) occurs and the molecule constitutes a dipole. Such push-pull systems are currently tremendously investigated as active molecules for nonlinear optics (NLO) and (opto)electronics.^{1, 2} Tripodal derived push-pull systems attract attention due to their two-photon absorption properties and thus resulting promising applications in microscopy, data storage, microfabrication or photodynamic therapy.³⁻⁵ Triphenylamine based compounds represent a (A- π)₃-D octupolar type of Y-shaped push-pull molecules featuring a central amino donor and three acceptor-substituted π -branches. For instance, the structure and electronic properties of metal-organic framework of triphenylamine molecules bearing π -deficient pyridine peripheral acceptors have been recently investigated.^{6, 7} It is well known that electron withdrawing ability of pyridine and related six-membered nitrogen-containing heterocyclic compounds can be improved by *N*-alkylation/protonation.⁸ Hence, in such molecules it would be very tempting to perform quaternization (ICT enhancement) in parallel with the structure ordering by incorporation into a system with confined geometry.⁹⁻¹¹ Materials prepared in such a way have the advantage, relative to organic hosts, of improved rigidity and thermal stability. An important class of these hybrid materials is intercalation compounds. These materials consist of layered solids (hosts), which contain other species (guests) between the layers, in the interlayer space. Restricted geometry in the interlayer space of layered inorganic solids helps to organize the incorporated species in a way favorable for the improvement of their optical properties.¹²

Up to now, only a few cases of intercalates with NLO properties has been reported.^{3, 10, 13, 14} As the host materials, mostly clays^{15, 16} and layered MPS₃ (M = Mn, Cd, Zn)^{9, 14} were used. In the case of cationic chromophores derived from stilbazolium intercalated into MPS₃, it is claimed that the confined interlayer space of the host lead to a chromophore aggregation.⁹ The formation of J aggregates has been reported to induce SHG properties because of the resulting noncentrosymmetric packing of the interacting chromophores.^{17, 18}

A host material with thoroughly studied intercalation chemistry is layered zirconium phosphate. This phosphate exists in two modifications: α -Zr(HPO₄)₂·H₂O and γ -Zr(PO₄)(H₂PO₄)·2H₂O. Both phosphates contain acidic OH groups, whose interaction with basic guest molecules serves as a driving force for the intercalations.¹⁹ Both zirconium phosphates are well transparent and their intercalation compounds with basic molecules are stable. An NLO active material made by intercalation of a (4'-(dimethylamino)-1-methylstilbazolium)⁺ cation into layered γ -ZrPO₄(H₂PO₄)·2H₂O phases has been reported by Coradin et al.²⁰ Another group of host materials is represented by zirconium phosphonates, derived from the phosphates by replacing the OH group with an organic rest.²¹ When such an organophosphonate is functionalized with an appropriate acidic group on the organic backbone, it can be used as a suitable host material. Recently, we have prepared zirconium 4-sulfophenylphosphonate with a general formula Zr(HO₃SC₆H₄PO₃)₂·yH₂O,²² and tested its intercalation ability.²³ Zirconium 4-sulfophenylphosphonate proved to be a very good host material for the intercalation of nitrogen-containing basic organic molecules.

In this paper we report on intercalation of tris[4-(pyridin-4-yl)phenyl]amine (**TPPA**) guest molecule into α -modification of zirconium phosphate and into zirconium 4-sulfophenylphosphonate. The prepared materials were characterized by thermogravimetry,

IR spectroscopy and powder X-ray diffraction. The presumed arrangement and electronic properties of the intercalated species are discussed.

Experimental

Synthesis of zirconium phosphate. Well-crystallized α modification of $\text{Zr}(\text{HPO}_4)_2 \cdot \text{H}_2\text{O}$ (further denoted as **ZrP**), was obtained according to the method proposed by Alberti and Torracca.²⁴ A clear solution was prepared by dissolving of $\text{ZrOCl}_2 \cdot 8\text{H}_2\text{O}$ (10.1 g), hydrofluoric acid (40% w/w, 8 mL) and H_3PO_4 (85% w/w, 92 mL) in water (160 mL). The solution was heated at 80°C for 4 days, maintaining a constant volume by continuously adding water. The **ZrP** precipitate was washed with de-ionized water and dried in air.

Synthesis of a ZrP intercalate with ϵ -aminocaproic acid. ϵ -Aminocaproic acid (further denoted as **ACA**) was intercalated by refluxing **ZrP** (10 g) in an aqueous solution of ϵ -aminocaproic acid (0.25 M, 400 mL) for 7 days. The solid product (further denoted as **ZrP·ACA**) was separated by filtration, washed with water and ethanol and dried in air. Its formula was determined to be $\text{Zr}(\text{HPO}_4)_2 \cdot (\text{H}_2\text{N}(\text{CH}_2)_5\text{COOH})_{0.80} \cdot 1.5\text{H}_2\text{O}$.²⁵

Preparation of a ZrP intercalate with tris[4-(pyridin-4-yl)phenyl]amine. The **ZrP·ACA** intercalate (0.05 g) was mixed with tris(4-(pyridin-4-yl)phenyl)amine (0.08 g) in water (9 mL). The mixture was placed into a Teflon-lined 23 mL Parr acid digestion bomb and heated under autogenous pressure at 130°C for about 20 hours. The product (further denoted as **ZrP·TPPA**) was separated by filtration, washed with water and dried in air. For the optical measurements the product was extracted in a Soxhlet extractor until the extract was colorless. Elemental analysis calcd./found for $\text{Zr}(\text{HPO}_4)_2 \cdot 0.21(\text{C}_{33}\text{H}_{24}\text{N}_4) \cdot 2.5\text{H}_2\text{O}$, $M_r = 428.30$; C, 19.43/19.85 \pm 0.04; H, 2.83/2.78 \pm 0.01; N, 2.75/2.69 \pm 0.02.

Synthesis of zirconium 4-sulfophenylphosphonate. Zirconium 4-sulfophenylphosphonate (further denoted as **ZrSPP**) was prepared according to the previously described procedure.²²

4-Sulfophenylphosphonic acid (2.38 g) and $\text{ZrOCl}_2 \cdot 8\text{H}_2\text{O}$ (2.58 g) were added to a mixture of 1M HF (50 mL) and 1M HCl (50 mL) in a 300-mL PP beaker. The reaction mixture was heated to 80 °C in an oil bath overnight during which time it evaporated to a half of volume. After that the mixture was evaporated to dryness at 80 °C. The solid was suspended in 1 M HCl and then centrifuged. This process was repeated three times and the obtained slurry was dried in a rotary evaporator at 70 °C to remove hydrochloric acid. The product was dried in a desiccator over NaOH. The sulfophenyl group is partially desulfonated during the synthesis, therefore the formula of the obtained product was $\text{Zr}(\text{HO}_3\text{SC}_6\text{H}_4\text{PO}_3)_{1.3}(\text{C}_6\text{H}_4\text{PO}_3)_{0.7} \cdot 2\text{H}_2\text{O}$.

Preparation of ZrSPP intercalate with tris[4-(pyridin-4-yl)phenyl]amine. Zirconium 4-sulfophenylphosphonate dihydrate (0.05 g) was mixed with tris[4-(pyridin-4-yl)phenyl]amine (0.08 g) in a mixture of water (6 mL) and ethanol (3 mL). The mixture was placed into a Teflon-lined 23 mL Parr acid digestion bomb and heated under autogenous pressure at 130°C for about 20 hours. The product was separated by filtration, washed with an ethanol-water mixture (1/2 v/v), then with ethanol and dried in air. For the optical measurements the product was extracted in a Soxhlet extractor until the extract was colorless.

Elemental analysis calcd./found for $\text{Zr}(\text{HO}_3\text{SC}_6\text{H}_4\text{PO}_3)_{1.3}(\text{C}_6\text{H}_4\text{PO}_3)_{0.7} \cdot 0.35(\text{C}_{33}\text{H}_{24}\text{N}_4) \cdot 2.5\text{H}_2\text{O}$, $M_r = 719.30$; C, 39.32/37.66±0.05; H, 3.28/2.86±0.01; N, 5.80/6.25±0.02; S, 5.80/6.25±0.03. The compound is in the further text denoted as **ZrSPP·TPPA**.

Powder X-ray diffraction data were obtained with a D8 Advance diffractometer (Bruker AXS, Germany) with Bragg-Brentano θ - θ geometry (40 kV, 30 mA) using $\text{CuK}\alpha$ radiation with secondary graphite monochromator. The diffraction angles were measured at room temperature from 2 to 70° (2θ) in 0.02° steps with a counting time of 15 s per step. Powder X-ray diffraction measurements at 210±1°C were carried out on a heated brass block

equipped with a thermocouple in the range from 2 to 35° (2θ) in 0.025° steps with a counting time of 15 s per step. The size of the crystallites of the intercalates was calculated according to the Scherrer formula²⁶ using an EVA software.²⁷

The thermogravimetric measurements (TGA) were done using a home-made apparatus constructed of a computer-controlled oven and a Sartorius BP210 S balance. The measurements were carried in air between 30 and 960 °C at a heating rate of 5 °C min⁻¹.

Infrared spectra in the range of 600–4000 cm⁻¹ were recorded at 64 scans per spectrum at 2 cm⁻¹ resolution using HATR adapter on a Perkin-Elmer FTIR Spectrum BX spectrometer on neat samples. All spectra were corrected for the presence of moisture and carbon dioxide in the optical path.

UV-Vis diffuse reflectance spectra of diluted (2 w/w % by Al₂O₃) powder materials were recorded in the range from 210 to 800 nm using UV-Vis Lambda 20 spectrometer (Perkin-Elmer, USA) equipped with a diffuse reflectance attachment with a 3-inch integrating sphere with Al₂O₃ as a reference. The reflectances were re-calculated using the Schuster–Kubelka–Munk equation, $F(R_{\infty}) = (1-R_{\infty})^2/2R_{\infty}$, where R_{∞} is the diffuse reflectance from a semi-infinite layer. For details see References.^{28, 29}

Results and discussion

Preparation and properties of TPPA/HTPPA/MeTPPA. Tris[4-(pyridin-4-yl)phenyl]amine (**TPPA**) guest molecule was prepared in a threefold Suzuki-Miyaura cross-coupling reaction of tris(4-iodophenyl)amine with pyridine-4-ylboronic acid (see also the ESI).^{6,7} This molecule possess three basic pyridine-4-yl (Py) groups that can easily be quaternized (Figure 1a). Whereas in the non-protonated **TPPA** molecule only a diminished ICT from the central amino donor to peripheral Py groups takes place, protonation/methylation of the Py groups afforded **HTPPA/MeTPPA** with significantly

enhanced electron withdrawing ability and ICT efficiency. *N*-Methyl derivative **MeTPPA** is chemically well-accessible by the reaction of **TPPA** with an excess of iodomethane. For its synthesis and full spectral characterization see the ESI. The enhanced charge-transfer in **HTPPA/MeTPPA** can be demonstrated by HOMO/LUMO localizations shown in Figure 1b.³⁰ The HOMO and LUMO are in both structures localized predominantly over one π -branch. Degenerated LUMO-1 and LUMO-2 were found on the remaining two branches. Whereas the HOMO/LUMO in **TPPA** are spread over the central amino donor and adjacent part of the 1,4-phenylene and Py moieties, in **HTPPA** are the HOMO and LUMO obviously separated on the central donor and peripheral acceptor. This indicates a significant charge-separation. Further electronic parameters of **TPPA** and **MeTPPA** are shown in Table 1.

Table 1. Experimental and calculated parameters of TPPA and MeTPPA.

Comp.	$E_{1/2(\text{ox1})/\text{HOMO}}$ [V/eV] ^a	$E_{1/2(\text{red1})/\text{LUMO}}$ [V/eV] ^a	λ_{max} [nm (eV)] ^b	E_{HOMO} [eV] ^c	E_{LUMO} [eV] ^c	ΔE [eV] ^c	β [10 ⁻³⁰ esu] ^c	γ [10 ⁻³⁹ esu] ^c
TPPA	1.08/-5.43	-	363 (3.42)	-8.29	-0.78	7.51	0.48	179284
MeTPPA	-	-1.11/-3.24	428 (2.90)	-7.39	-2.28	5.11	4.87	692195

^a $E_{1/2(\text{ox1})}$ and $E_{1/2(\text{red1})}$ are the half-wave potentials of the first oxidation and reduction, respectively, as measured by RDV; $E_{\text{HOMO/LUMO}}^{\text{abs}} = E_{1/2(\text{ox1/red1})} + 4.35$. ^bLongest-wavelength absorption maxima measured in CH₃OH ($c = 2 \times 10^{-5}$ M). ^cCalculated by MOPAC 2012.

Electrochemical measurements carried out in DMF containing 0.1 M Bu₄NPF₆ in a three electrode cell by cyclic voltammetry (CV) and rotating disc voltammetry (RDV) or polarography. The first oxidation and reduction potentials $E_{1/2(\text{ox1})}$ and $E_{1/2(\text{red1})}$ are shown in Table 1. Unfortunately, the first reduction/oxidation potentials of **TPPA** and **MeTPPA**, respectively, are out of the potential window available in DMF and Pt electrode. However,

when going from **TPPA** to **MeTPPA**, the calculated HOMO-LUMO gaps decreased from 7.51 to 5.11 eV. This is mainly caused by raised HOMO and decreased LUMO in **MeTPPA** by 0.90 and 1.50 eV. In addition, positions of the longest-wavelength absorption maxima λ_{\max} (CT-bands) measured in CH₃OH (see the ESI) showed significant bathochromic shift from 363 to 428 nm ($\Delta\lambda_{\max} = 65$ nm) as a result of better D-A interaction in **MeTPPA**. The calculated ground state dipole moments of both molecules are nearly zero due their centrosymmetry. Hence, the observed enhancement in the calculated first hyperpolarizability β from 0.48 to 4.87×10^{-30} esu must be elucidated as a change in the spatial electron distribution in **MeTPPA**. The second hyperpolarizability γ increased from 179284 (**TPPA**) to 692195×10^{-39} esu (**MeTPPA**).

Characterization of the intercalates. The **ZrP·TPPA** intercalate shows a weight decrease of 10% on heating to about 200°C (Figure 2). This corresponds to a release of 2.5 molecules of water per formula unit (theoretical weight loss is 10%). Further steep decrease of weight at around 500°C is due to the deintercalation of the amine. The total weight loss observed to 980°C is 36%, which is close to the theoretical weight loss (37%) calculated for ZrP₂O₇ as the final product of the heating, considering the amount of the intercalate to be 0.21 per formula unit.

The **ZrSPP·TPPA** intercalate is slightly less stable than **ZrP·TPPA**, as can be seen from the comparison of their thermogravimetric curves (Figure 2). Also for **ZrSPP·TPPA** the first step of the weight loss of 6% corresponds to the release of water from the interlayer space. The further decomposition of the intercalate starts about 400°C and is caused by the deintercalation of the amine and decomposition of the organic part of sulfophenylphosphonate. The total weight loss is 66%, which indicates the formation of

ZrP₂O₇ as a final product (theoretical weight loss of 63%, considering the amount of the intercalated **TPPA** to be 0.35, as given in the Experimental).

Infrared spectra. The way of interaction between the host material and the intercalated species was also studied by infrared spectra, shown in Figures 3 and 4 for **ZrP** and **ZrSPP** as the hosts, respectively.

The distinct couple of bands at 3588 and 3507 cm⁻¹ found in **ZrP** and corresponding to stretching vibrations of the PO-H bond³¹ is replaced by a broad band both in the aminocaproic acid preintercalated host (**ZrP·ACA**) and the final **ZrP·TPPA** intercalate. Also the band at 3112 cm⁻¹ corresponding to O-H stretching vibration of water molecules observed in **ZrP** is broadened in both **ZrP·ACA** and **ZrP·TPPA**. The intensive band at 1704 cm⁻¹, corresponding to C=O stretching vibrations of the carboxylic group, which appears after the intercalation of aminocaproic acid, is not present in the **ZrP·TPPA**. This is evidence that all **ACA** was replaced by **TPPA**.

To determine, whether the **TPPA** guest is present in the intercalate as a protonated or neutral species, the IR spectra of **TPPA** and its methylpyridinium derivative (tris(4-(N-methylpyridinium-4-yl)phenyl)amine, **MeTPPA**) were also measured. The most distinct difference between the IR spectra of **TPPA** and **MeTPPA** is a triple of ring stretching vibrations at 1585, 1517, and 1484 cm⁻¹ in **TPPA**, which are in **MeTPPA** shifted to 1637, 1581, and 1492 cm⁻¹. These bands are characteristic for aromatic compounds, the observed shift to a higher energy region corresponds to the significantly higher polarization of the **MeTPPA** molecules having a ⁺NMe terminus. It was found that this shift occurs also in partially protonated **TPPA**.

In **ZrP·TPPA** these bands are at the same positions (1637, 1594, and 1492 cm⁻¹) as in **MeTPPA**, which confirms that the **TPPA** guest molecules are present in the intercalate in a protonated form. The H-O-H deformation vibration of water molecules observed in **ZrP** and

in **ZrP·ACA** is in the **ZrP·TPPA** intercalate most probably masked by the ring stretching vibration bands. The C-H deformation vibration bands present at 1335, 1295, 1230, and 1185 cm^{-1} in **MeTPPA** are very poorly developed in **ZrP·TPPA**. The P-O-H deformation vibration present in **ZrP** at 1247 cm^{-1} is strongly suppressed in **ZrP·TPPA**. A broad and intensive band between 1150 and 900 cm^{-1} belongs to P-O antisymmetric stretching vibrations and P-OH stretching vibrations of the host. In the intercalate as in the guest spectra, there is a distinct band at 820 cm^{-1} of a C-H deformation vibration typical for *para*-substituted benzene derivatives.

In the IR spectrum of **ZrSPP** (see Figure 4), there is a very weak band at 1386 cm^{-1} corresponding to aromatic C-C ring stretching vibrations. More distinct band at 1152 cm^{-1} is given by P-O asymmetric stretching vibrations and the most intensive and broad couple of bands appearing at 1039 and 1007 cm^{-1} corresponds to P-O and S-O vibrations. The band at 831 cm^{-1} arises due to 1,4-disubstituted benzene ring vibrations and the band observed at 653 cm^{-1} reflects C-S vibrations of the sulfonic group. All these bands can be observed also in the IR spectrum of **ZrSPP·TPPA**. In addition a distinct triple of bands at 1636, 1594, 1490 cm^{-1} and less distinct bands at 1328, 1290, 1216 together with a shoulder at 1180 cm^{-1} are bands characteristic of **MeTPPA**.

In summary, the infrared spectra of both **ZrP·TPPA** and **ZrSPP·TPPA** indicate that the **TPPA** guest is present in its protonated form in the intercalates.

Powder patterns of the intercalates. On intercalation, a distinct enlargement of the interlayer distance was observed for both host materials, see Figures 5 and 6.

The interlayer distance for the **ZrP·TPPA** intercalate increased to 18.52 Å (Figure 5) from the original interlayer distance of 7.6 Å in the host material. The peak at $2\theta = 33.8^\circ$ corresponding to the 020 reflection is distinct in the original **ZrP** host but is broadened in **ZrP·TPPA** due to the lower crystallinity of the intercalate. Nevertheless, the fact that this 020

reflection is retained in **ZrP** confirms that the structure of the **ZrP** host is retained in the intercalate. It was reported, that the layer thickness of **ZrP** is 6.3 Å.¹⁹ It means that the height of the interlayer space (gallery) in the **ZrP·TPPA** intercalate is 18.5 - 6.3 = 12.2 Å. In the case of the **ZrSPP·TPPA** intercalate, the layer thickness (taken as the distance between the sulfo oxygen atoms of one side of the **ZrSPP** layer to the sulfo oxygen atoms on the other side) was determined to be 16.8 Å,²³ and the interlayer distance in the **ZrSPP·TPPA** intercalate is 33.2 Å (see Figure 6). Thus, the height of the gallery in this intercalate is 33.2 - 16.8 = 16.4 Å. The size of the crystallites determined from powder X-ray diffraction is 244 Å for **ZrP·TPPA** and 325 Å for **ZrSPP·TPPA**.

Geometrical considerations on the intercalates. The **TPPA** molecule has a shape of an equilateral triangle with the height of roughly 16.2 Å (see Figure 7a). We can consider the arrangement of the **TPPA** molecules in the interlayer space of the host in the following ways: (a) The molecules are placed parallel to the plane of the host layers as monomolecular sheets. In such a case the height of the interlayer space (gallery) should be about 4 Å. (b) The molecules are placed parallel with the host layers in a bimolecular way that is there are two sheets of the **TPPA** molecules placed above each other in the gallery. In such a case the gallery height should be 8 Å. Presence of more sheets of **TPPA** molecules in the gallery is improbable, as in such an arrangement the **TPPA** molecules should be bonded very loosely to the host layers. (c) The **TPPA** molecules are placed perpendicularly to the plane of the host layers. In the most probable arrangement, the **TPPA** molecule is placed so that one of its sides lies on the plane of the host layer while with its remaining corner it is bonded to the neighboring host layer. Then the gallery height should be close to the value given in Figure 7a, i.e. 16.2 Å.

The actual enlargement of the interlayer space on the intercalation of **TPPA** into **ZrP** is larger than in the cases (a) and (b) but lower than in the case (c). It means that the **TPPA** molecules

are placed in the interlayer space of **ZrP** in the manner described for (c) but with a slightly slanting position. In the case of the **ZrSPP·TPPA** intercalate, the gallery height determined by powder XRD (16.4 Å) is slightly higher than the height of the **TPPA** molecule (16.2 Å). Therefore, in this case we can presume that the **TPPA** molecules are oriented perpendicularly to the host layers of **ZrSPP**.

Let us discuss the way the molecules are placed *on* the host layers; this way influences the amount of the intercalated **TPPA** molecules and consequently also the amount of water present in the intercalate. In the alpha modification of $\text{Zr}(\text{HPO}_4)_2$ the acidic OH groups of the phosphates are placed uniformly above and below the host layers in an equilateral triangular fashion (see Figure 7b) with the in-plane distance between them of about 5.3 Å.

The driving force for the intercalation process in **ZrP** is a proton transfer from the host HPO_4 group to the intercalated amine. During the intercalation the pyridine nitrogen atoms are protonated, while the OH groups of the phosphate are deprotonated. If we presume the arrangement of the **TPPA** molecule as that described in case (c) above, then distance of nitrogen atoms in **TPPA** lying on the host plane is about 14.7 Å. The protonated nitrogen atoms should be as close to the acidic oxygen atoms of the phosphate groups as possible. This condition can be fulfilled when the **TPPA** molecules are placed on the host layer in a manner shown in Figure 7b.

In **ZrSPP** we presumed that its structure is derived from the structure of alpha modification of **ZrP**, with OH phosphate groups being replaced by $\text{C}_6\text{H}_4\text{SO}_3\text{H}$ groups, which are oriented perpendicularly to the inorganic sheets of the Zr atoms.²³ It means that the SO_3H groups of the host are placed uniformly at the surface of the host layers in an equilateral triangular fashion as the OH groups in **ZrP**. Similarly to **ZrP**, the driving force for the intercalation in **ZrSPP** is a proton transfer from the SO_3H group to the pyridine nitrogen atoms.

From the structure of **ZrP** it follows that on the surface of the host layer there is a “free area” of 24 \AA^2 associated to each phosphate group.¹⁹ Thus, for each $\text{Zr}(\text{HPO}_4)_2$ formula unit we have $2 \times 24 = 48 \text{ \AA}^2$ free area which can be covered with the guest. Let us consider that the triangular **TPPA** molecule is anchored to one layer of **ZrP** by its base (side) and to the another neighboring layer by its apex (corner). Cross section of the base (the area which is covered by this part of the **TPPA** molecule) is about 116 \AA^2 . Cross section at the apex of **TPPA** is about 21 \AA^2 . In summary, the area covered by the **TPPA** molecule in **ZrP·TPPA** is therefore $0.21 \times (116 + 21) = 29 \text{ \AA}^2$, which is an area much smaller than that provided by the **ZrP** host. In case of **ZrSPP·TPPA**, the area covered by the **TPPA** molecule is $0.35 \times (116 + 21) = 48 \text{ \AA}^2$, which indicates that the whole surface of the **ZrSPP** layer is covered by the guest molecules. Therefore the amount of **TPPA** intercalated into **ZrSPP** (0.35 per formula unit) represents the maximum amount which can be intercalated into this type of the host due to the sterical reasons.

The van der Waals volume of the **TPPA** molecule calculated by a Hyperchem software³² is 462 \AA^3 . The molecule geometry was optimized by PM3 and PM7 semi-empirical methods implemented in programs ArgusLab³³ and MOPAC2012.³⁴ The volume accessible for the intercalated entities might be calculated as the “free area” (24 \AA^2) multiplied by the gallery height. Thus for the **ZrP·TPPA** the accessible volume is $24 \times 12.2 = 293 \text{ \AA}^3$ and for **ZrSPP·TPPA** it is $24 \times 16.4 = 394 \text{ \AA}^3$. In **ZrP·TPPA**, there is 0.21 molecules of **TPPA** per formula unit, and the space occupied by **TPPA** is therefore $0.21 \times 462 = 97 \text{ \AA}^3$ and in **ZrSPP·TPPA** it is $0.35 \times 462 = 162 \text{ \AA}^3$. In both cases there is enough space for water molecules to be placed among the **TPPA** molecules.

Thermal behavior of the intercalates. On heating the interlayer distance decreases in both intercalates (see Figures S4 and S5 in the ESI). In case of **ZrP·TPPA** the interlayer distance

decreases from 18.5 Å at room temperature to 16.6 Å at 210°C. In case of **ZrSPP·TPPA**, this decrease is from 33.2 to 31.5 Å. The change of the interlayer distance can be explained by the release of water. The empty space formed after the dehydration allows further slanting of the **TPPA** molecules in the intercalate resulting in a decrease of the interlayer distance.

The intercalates might be rehydrated. In the case of **ZrP·TPPA** intercalate a rehydration by standing the sample at 25-30% of relative humidity (RH) and at room temperature for 24 h causes an increase of the interlayer distance to 17.2 Å. The full rehydration close to the original state (18.44 Å) was achieved by standing the sample at room temperature at 100% RH for another 24 h. The rehydration of the **ZrSPP·TPPA** sample was, on the other hand, easier, because standing the sample at room temperature at 25-30% RH for 24 h was sufficient to achieve the original value of the interlayer distance.

UV-Vis spectra of the intercalates. Figure 8 shows UV-Vis spectra of **TPPA**, **MeTPPA**, **ZrP·TPPA** and **ZrSPP·TPPA**. From the comparison of the spectra of **TPPA**, **MeTPPA** and those of the intercalates it follows that both intercalates contain **TPPA** both in protonated and deprotonated forms in an equilibrium. This finding is in discrepancy with the results of the IR spectra measurements, where the bands of deprotonated **TPPA** were not found in the IR spectra of **ZrP·TPPA** and **ZrSPP·TPPA**. To solve this problem, we measured IR spectra of partially protonated **TPPA**. We prepared a solution of 1 mol of **TPPA** with 1.5 mol of HCl so that **TPPA** (with three protonable pyridine groups) would be protonated to one half. The IR spectrum of the resulting product (see Figure S6c in the ESI) is different from that of **TPPA** and corresponds to the spectrum of **MeTPPA**. Thus both the UV-Vis and IR spectra confirm that the **TPPA** guest in **ZrP·TPPA** and **ZrSPP·TPPA** is partially protonated.

Deconvolution of the longest-wavelength absorption maxima λ_{\max} of **ZrP·TPPA** and **ZrSPP·TPPA** (see Figure S7 in the ESI) revealed two peaks appearing at ~370 and 450 nm that fit the positions of CT-peaks of **TPPA** and **MeTPPA** (Figure 8). The observed

bathochromic shift with $\Delta\lambda_{\max} \sim 80$ nm is similar to that observed in the solution (see above) and indicates enhanced ICT in both intercalates. In the case of **ZrP·TPPA** the shape of the spectrum suggests that the deprotonated form is present in the intercalate in a higher relative amount than in **ZrSPP·TPPA**. This further implies that the interlayer environment of the **ZrSPP** host is more acidic than that of **ZrP**. The question arises whether this partially protonated **TPPA** in the intercalates might be further protonated by exposing the intercalates to an acidic environment. When the **ZrP·TPPA** and **ZrSPP·TPPA** intercalates are subjected to HCl vapors overnight, their UV-Vis spectra change distinctly and are identical with that of **MeTPPA** (see Figure S8 in the ESI for **ZrP·TPPA**). The powder XRD pattern of **ZrP·TPPA** after the exposition is identical with that before exposition. It means that no deintercalation occurred in this case. On the other hand, the powder XRD pattern of **ZrSPP·TPPA** after the exposition is identical with that of **ZrSPP**; it means the **TPPA** guest molecules are deintercalated in an acidic environment.

Conclusion

Tris[4-(pyridin-4-yl)phenyl]amine was successfully intercalated into α -modification of zirconium phosphate and into zirconium 4-sulfophenylphosphonate. It was found that the guest amine is protonated during the intercalation on the peripheral pyridine-4-yl moieties. The UV-Vis spectra suggested an equilibrium between the protonated and non-protonated forms of the amine. However, a significant bathochromic shift and thus an ICT enhancement were revealed in the solution as well as in the solid state. This is further supported by the electrochemical measurements and calculations of further electronic properties for both limit **TPPA** and **MeTPPA** structures. Based on the amount of the intercalated species and the enlargement of the interlayer space caused by the intercalation the probable arrangement of the molecules of the guest in the intercalate was suggested. The triangular shape of the guest

molecule leaves enough space between the layers of the host, so that water molecules can be accommodated in the interlayer space at ambient conditions. On heating the water is released from the intercalate and, as a consequence of this release, the interlayer distance in the intercalate decreases, which is caused by a reorientation (slanting) of the guest molecules with respect to the host layers. The prepared materials represent the first example of tripodal push-pull organic molecules introduced in a confined space of layered materials with the aim to influence their optical properties. In view of the current interest in novel inorganic-organic hybrid materials, this structure-property relationships study would serve as a useful guide for designing new intercalates with tunable optical properties.

Acknowledgements

The authors thank the Czech Science Foundation (grant No. 13-01061S) for the financial support.

Figure captions

Figure 1 Quaternization of **TPPA** and its impact on the ICT (a) and HOMO (red) and LUMO (blue) localizations in **TPPA** and **HTPPA**, respectively (b). Counter ions were omitted for clarity.

Figure 2 Thermogravimetric curves of **ZrP·TPPA** (a) and **ZrSPP·TPPA** (b) intercalates.

Figure 3 Infrared spectra of **TPPA** (a), **MeTPPA** (b), **ZrP·TPPA** (c), **ZrP** (d), and **ZrP·ACA** (e).

Figure 4 Infrared spectra of **TPPA** (a), **MeTPPA** (b), **ZrSPP·TPPA**, and **ZrSPP** (d).

Figure 5 Diffraction patterns of the host **ZrP** material (a), and its intercalate with **TPPA** (b)

Figure 6 Diffraction patterns of the host **ZrSPP** (a), and its intercalate with **TPPA** (b).

Figure 7 The **TPPA** molecule and its dimension (a). The placement of the **TPPA** molecules on the host layer (b).

Figure 8 UV-Vis spectra of **TPPA** (a), **MeTPPA** (b), **ZrP·TPPA** (c), **ZrSPP·TPPA** (d).

References

1. S. R. Forrest and M. E. Thompson, *Chem. Rev.*, 2007, **107**, 923-925.
2. R. D. Miller and E. A. Chandross, *Chem. Rev.*, 2010, **110**, 1-2.
3. Y. Suzuki, Y. Tenma, Y. Nishioka and J. Kawamata, *Chem.-Asian J.*, 2012, **7**, 1170-1179.
4. O. V. Przhonska, S. Webster, L. A. Padilha, H. Hu, A. D. Kachkovski, D. J. Hagan and E. W. v. Stryland, in *Advanced Fluorescence Reporters in Chemistry and Biology I: Fundamentals and Molecular Design*, ed. A. P. Demchenko, *Springer Ser. Fluoresc.* 2010, **8**, 105-148.
5. W. H. Lee, H. Lee, J. A. Kim, J. H. Choi, M. H. Cho, S. J. Jeon and B. R. Cho, *J. Am. Chem. Soc.*, 2001, **123**, 10658-10667.
6. M. D. Zhang, C. M. Di, L. Qin, X. Q. Yao, Y. Z. Li, Z. J. Guo and H. G. Zheng, *Cryst. Growth Des.*, 2012, **12**, 3957-3963.
7. C. Hua, P. Turner and D. M. D'Alessandro, *Dalton Trans.*, 2013, **42**, 6310-6313.
8. M. A. Ramirez, R. Custodio, A. M. Cuadro, J. Alvarez-Builla, K. Clays, I. Asselberghs, F. Mendicuti, O. Castano, J. L. Andres and J. J. Vaquero, *Org. Biomol. Chem.*, 2013, **11**, 7145-7154.
9. T. Coradin, R. Clement, P. G. Lacroix and K. Nakatani, *Chem. Mater.*, 1996, **8**, 2153-2158.
10. M. Ogawa and K. Kuroda, *Chem. Rev.*, 1995, **95**, 399-438.
11. M. Ogawa, *J. Mater. Chem.*, 2002, **12**, 3304-3307.
12. P. Lacroix, *Chem. Mater.*, 2001, **13**, 3495-3506.
13. J. S. O. Evans, S. Benard, P. Yu and R. Clement, *Chem. Mater.*, 2001, **13**, 3813-3816.
14. S. Benard, A. Leautic, E. Riviere, P. Yu and R. Clement, *Chem. Mater.*, 2001, **13**, 3709-3716.
15. R. Takenawa, Y. Komori, S. Hayashi, J. Kawamata and K. Kuroda, *Chem. Mater.*, 2001, **13**, 3741-3746.
16. M. Ogawa, M. Takahashi and K. Kuroda, *Chem. Mater.*, 1994, **6**, 715-717.
17. V. Mizrahi, G. I. Stegeman and W. Knoll, *Phys. Rev. A*, 1989, **39**, 3555-3562.
18. R. Steinhoff, L. F. Chi, G. Marowsky and D. Mobius, *J. Opt. Soc. Am. B-Opt. Phys.*, 1989, **6**, 843-847.
19. A. Clearfield and U. Costantino, in *Comprehensive Supramolecular Chemistry*, eds. G. Alberti and T. Bein, Pergamon Press, Oxford, 1996, vol. 7, pp. 107-149.
20. T. Coradin, R. Backov, D. J. Jones, J. Roziere and R. Clement, *Mol. Cryst. Liq. Cryst. Sci. Technol. Sect. A-Mol. Cryst. Liq. Cryst.*, 1998, **311**, 275-280.
21. G. Alberti, in *Comprehensive Supramolecular Chemistry*, eds. G. Alberti and T. Bein, Pergamon Press, Oxford, 1996, vol. 7, pp. 151-187.
22. V. Zima, J. Svoboda, K. Melánová, L. Beneš, M. Casciola, M. Sganappa, J. Brus and M. Trchová, *Solid State Ionics*, 2010, **181**, 705-713.
23. J. Svoboda, V. Zima, K. Melánová, L. Beneš and M. Trchová, *J. Solid State Chem.*, 2013, **208**, 58-64.
24. G. Alberti and E. Torracca, *J. Inorg. Nucl. Chem.*, 1968, **30** 317-318.
25. Y. Ding, D. J. Jones, P. Maireles-Torres and J. Roziere, *Chem. Mater.*, 1995, **7**, 562-571.
26. A. Patterson, *Phys. Rev.*, 1939, **56**, 978-982.
27. EVA, ver.19., Diffrac plus Basic Evaluating Package, Bruker AXS GmbH, Germany, 2013.
28. P. Knotek, L. Capek, R. Bulanek and J. Adam, *Top. Catal.*, 2007, **45**, 51-55.

29. R. Bulanek, P. Cicmanec, H. Sheng-Yang, P. Knotek, L. Capek and M. Setnicka, *Appl. Catal. A-Gen.*, 2012, **415**, 29-39.
30. OPchem, O. Pytela, version 6.2, webpage: <http://pytela.upce.cz/OPgm>.
31. P. L. Stanghellini, E. Boccaleri, E. Diana, G. Alberti and R. Vivani, *Inorg. Chem.*, 2004, **43**, 5698-5703.
32. Hyperchem, Computational Chemistry, Hypercube Inc., Gainesville, USA, Hyperchem Release 5. Standalone version, 1996.
33. ArgusLab, Mark Thompson and Planaria Software LLC, Version 4.01, webpage: <http://www.arguslab.com>.
34. MOPAC2012, J. J. P. Stewart, Stewart Computational Chemistry, version 13.084W, webpage: <http://OpenMOPAC.net>.

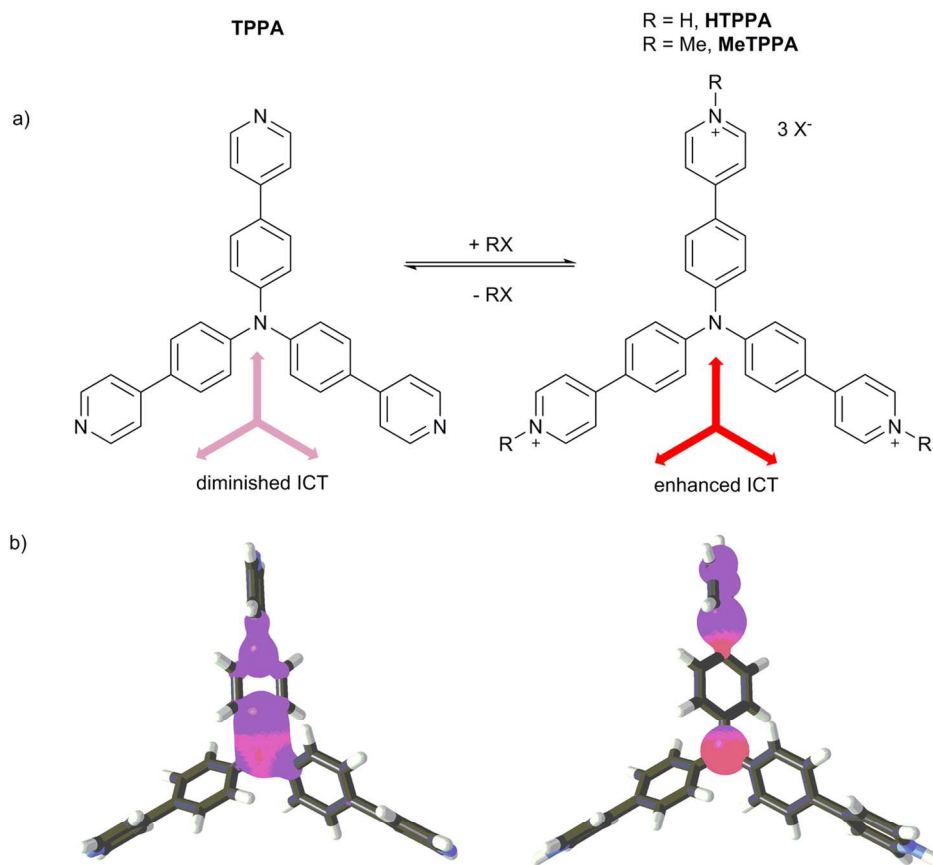


Figure 1 Quaternization of TPPA and its impact on the ICT (a) and HOMO (red) and LUMO (blue) localizations in TPPA and HTPPA, respectively (b). Counter ions were omitted for clarity.
127x130mm (300 x 300 DPI)

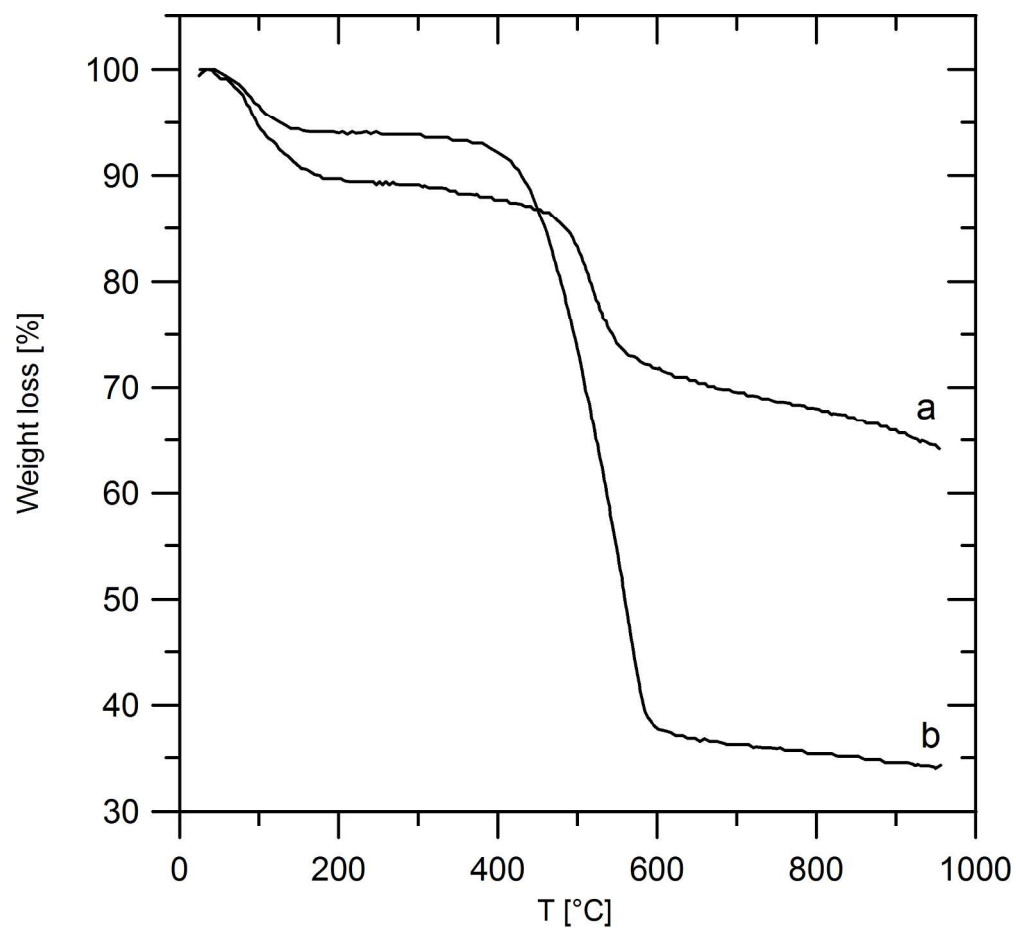


Figure 2 Thermogravimetric curves of ZrP·TPPA (a) and ZrSPP·TPPA (b) intercalates.
191x174mm (300 x 300 DPI)

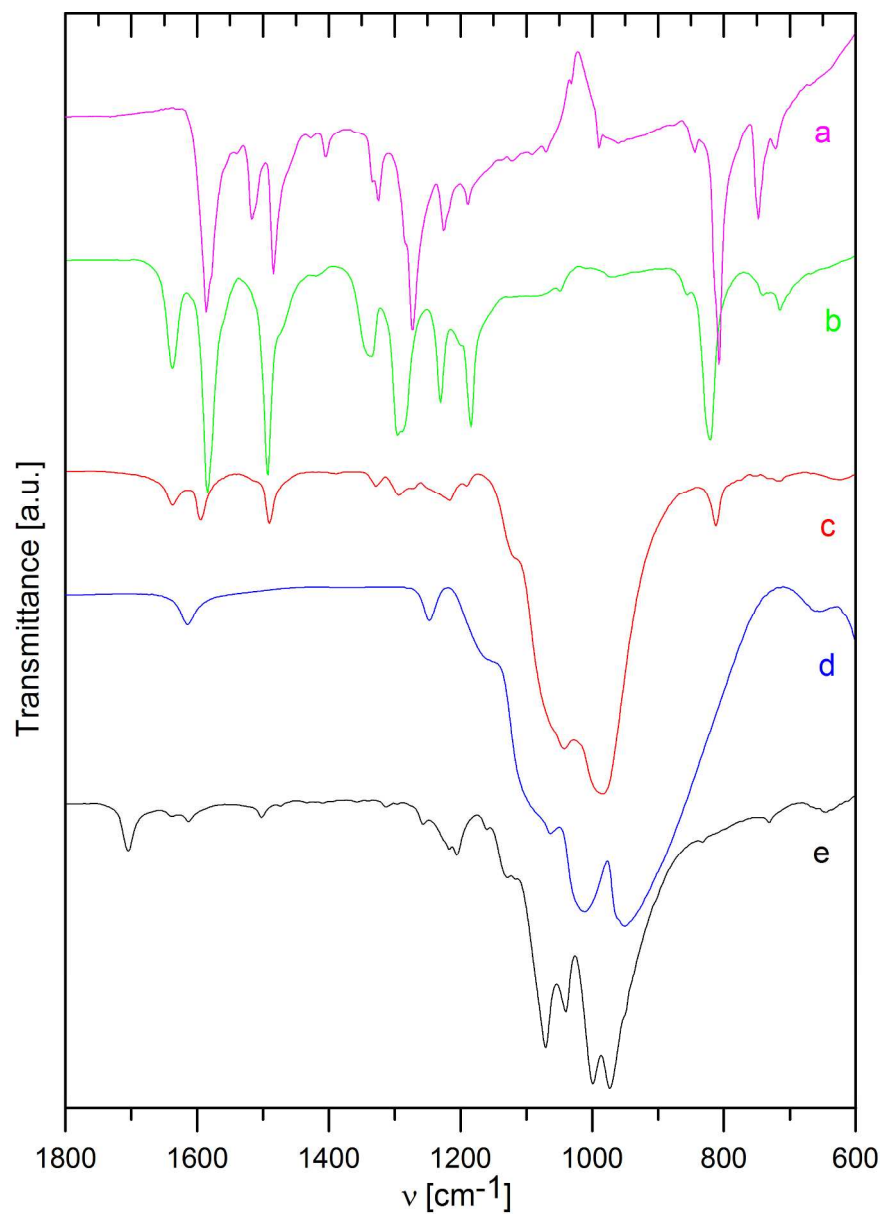


Figure 3 Infrared spectra of TPPA (a), MeTPPA (b), ZrP·TPPA (c), ZrP (d), and ZrP·ACA (e).
195x270mm (300 x 300 DPI)

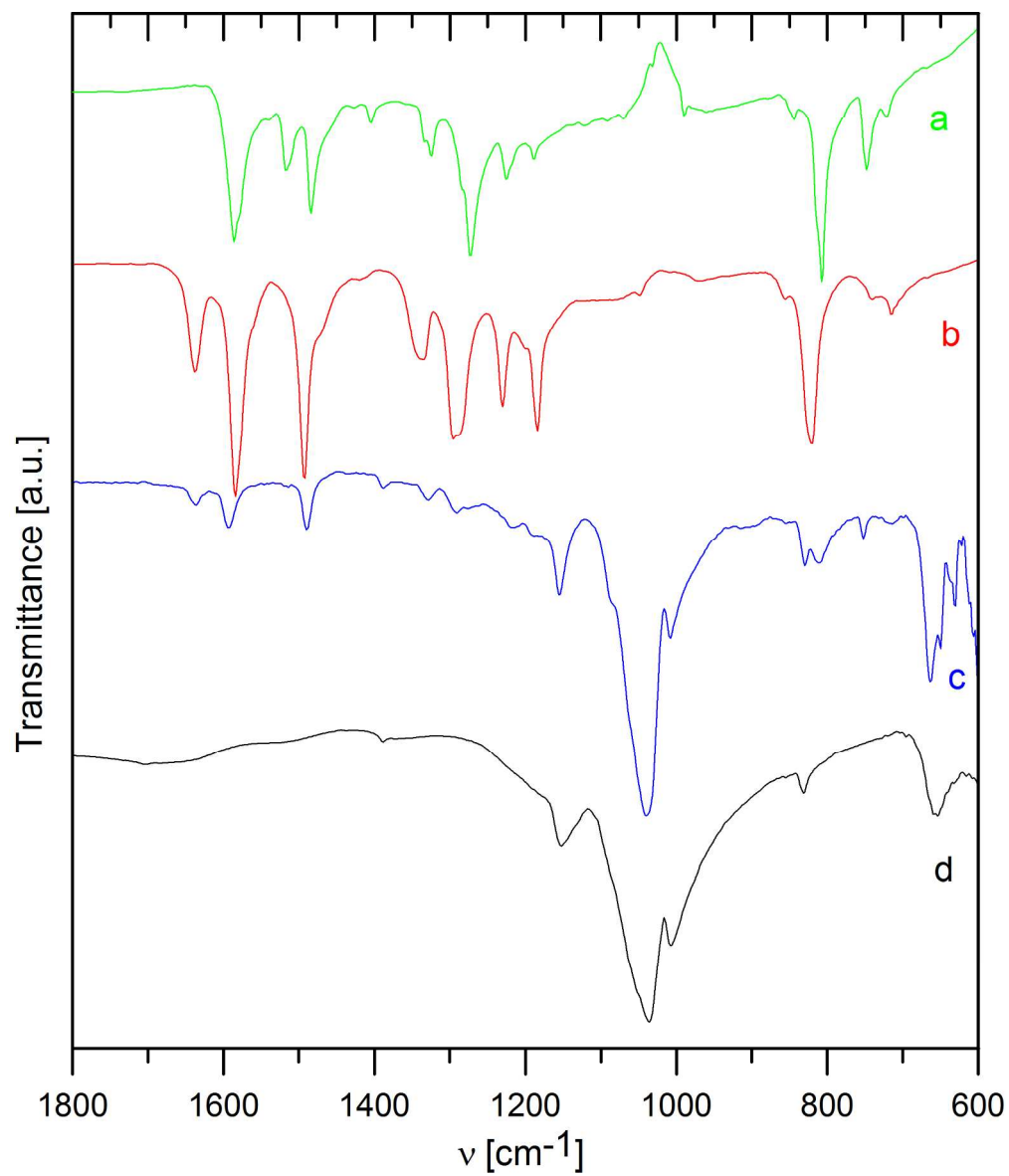


Figure 4 Infrared spectra of TPPA (a), MeTPPA (b), ZrSPP·TPPA, and ZrSPP (d).
195x227mm (300 x 300 DPI)

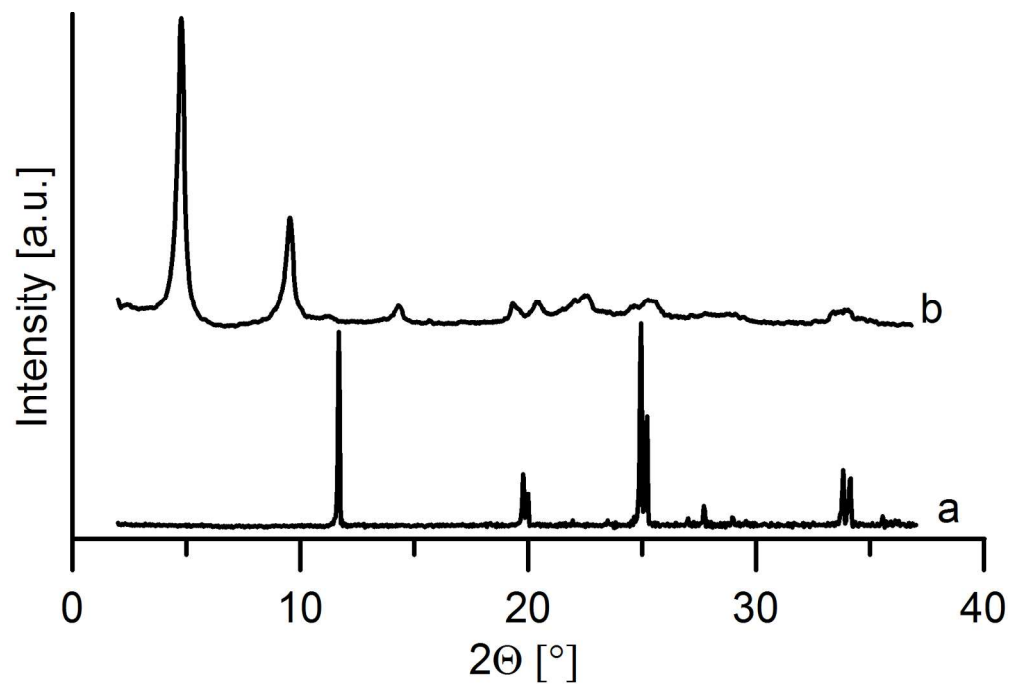


Figure 5 Diffraction patterns of the host ZrP material (a), and its intercalate with TPPA (b)
167x112mm (300 x 300 DPI)

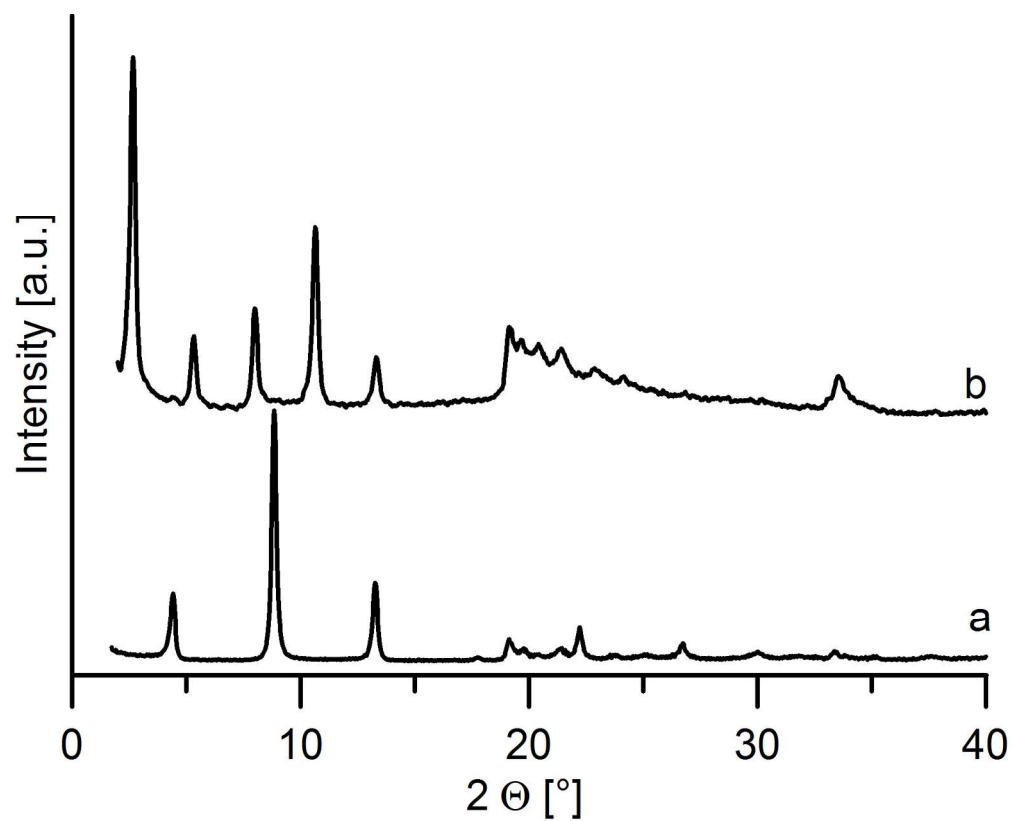


Figure 6 Diffraction patterns of the host ZrSPP (a), and its intercalate with TPPA (b).
167x134mm (300 x 300 DPI)

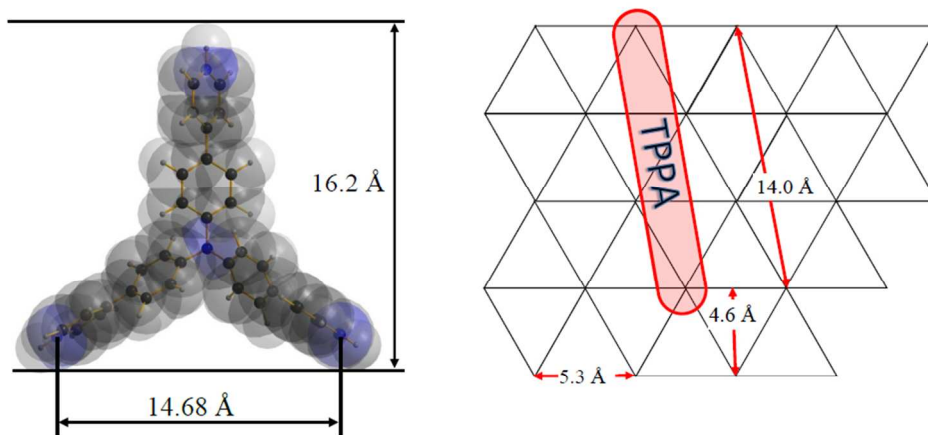


Figure 7 The TPPA molecule and its dimension (a). The placement of the TPPA molecules on the host layer (b).
354x167mm (72 x 72 DPI)

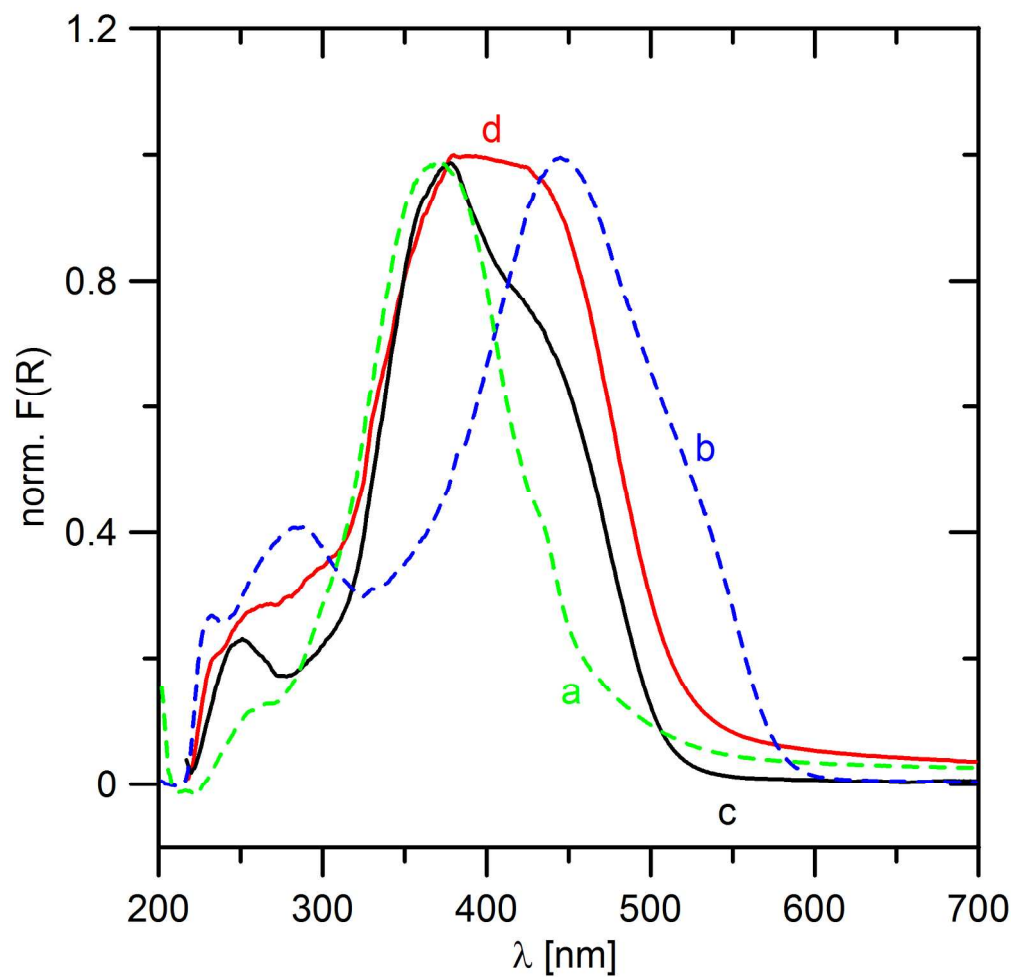
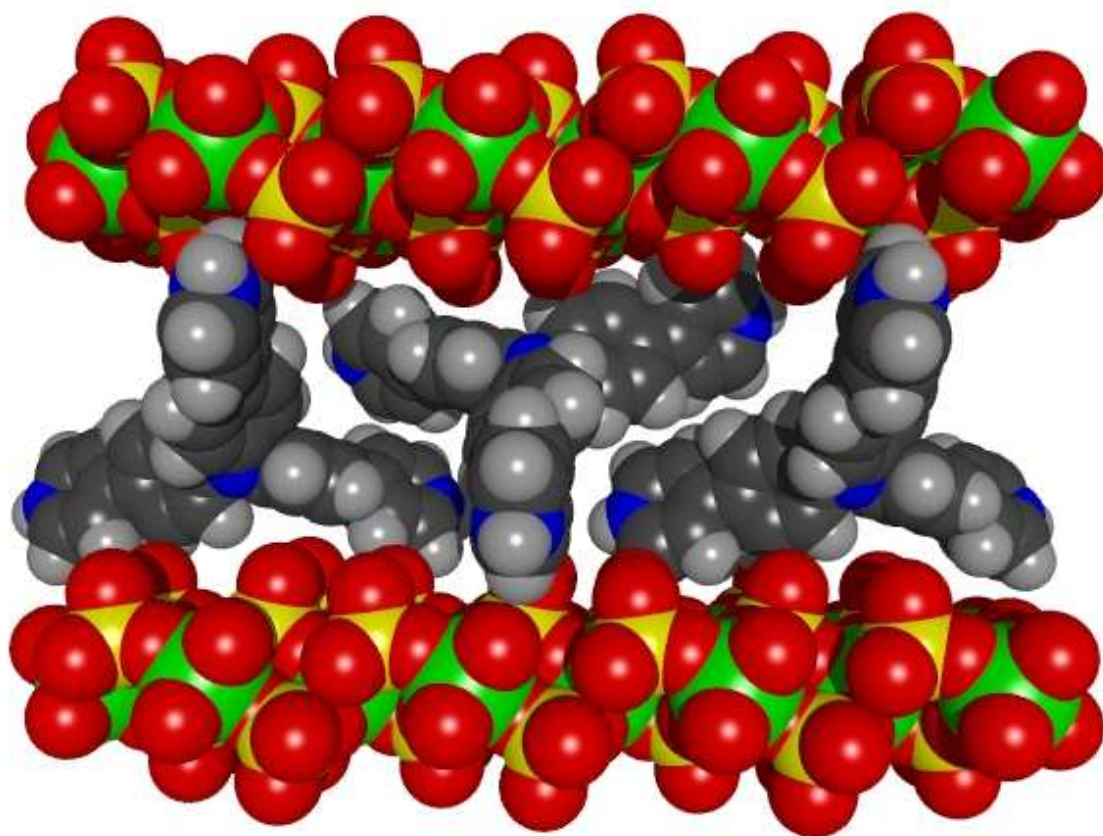


Figure 8 UV-Vis spectra of TPPA (a), MeTPPA (b), ZrP-TPPA (c), ZrSPP-TPPA (d).
186x180mm (300 x 300 DPI)

Graphical abstract



Intercalation of tripodal tris[(pyridine-4-yl)phenyl]amine push-pull molecules into zirconium phosphate and zirconium 4-sulfophenylphosphonate leads to their organization in a layered system of the hosts.